ARTICLE

Check for updates

Observation of a flat band and bandgap in millimeter-scale twisted bilayer graphene

Keiju Sato[1,2], Naoki Hayashi[1], Takahiro Ito[3], Noriyuki Masago[2], Makoto Takamura[2], Mitsuru Morimoto[2], Takuji Maekawa[2], Doyoon Lee [4], Kuan Qiao[4], Jeehwan Kim [4], Keisuke Nakagahara[5], Katsunori Wakabayashi [5], Hiroki Hibino[5] & Wataru Norimatsu [1✉]

Magic-angle twisted bilayer graphene, consisting of two graphene layers stacked at a special angle, exhibits superconductivity due to the maximized density of states at the energy of the flat band. Generally, experiments on twisted bilayer graphene have been performed using micrometer-scale samples. Here we report the fabrication of twisted bilayer graphene with an area exceeding 3×5 mm^2 by transferring epitaxial graphene onto another epitaxial graphene, and observation of a flat band and large bandgap using angle-resolved photoemission spectroscopy. Our results suggest that the substrate potential induces both the asymmetrical doping in large angle twisted bilayer graphene and the electron doped nature of the flat band in magic-angle twisted bilayer graphene.

[1] Department of Materials Science and Engineering, Nagoya University, Nagoya 464-8603, Japan. [2] Research and Development Center, ROHM Co., Ltd., 615-8585 Kyoto, Japan. [3] Synchrotron Radiation Research Center, Nagoya University, Nagoya 464-8603, Japan. [4] Department of Mechanical Engineering, Massachusetts Institute of Technology, Cambridge, MA 02139, USA. [5] School of Science and Technology, Kwansei Gakuin University, Hyogo 669-1337, Japan
. ✉email: norimatsu.wataru@material.nagoya-u.ac.jp

Various approaches have been attempted to modify the electronic structure of the graphene system for a wide variety of applications. In twisted bilayer graphene (TBG), the electronic structure can be modified by changing the rotation angle θ[1,2]. The interlayer interaction in TBG introduces interference between two Dirac cones, resulting in the bandgap and flat band[3]. In addition, TBG with a small rotation angle exhibits a superstructure, that produces a moiré pattern[4]. A periodic potential such as this moiré superstructure also modifies the band structure[5–8]. Twisting the layers is a fascinating technique to introduce another direction to electronic structure modification, not only in graphene, but also in other two-dimensional materials, a phenomenon which has become known as twistronics[9].

The most striking experimental results reported on this subject were the observation of superconductivity in "magic-angle" ($\theta = 1.1°$) TBG[10,11]. The physical origin of the superconductivity is the flat band at the Fermi energy, leading to a maximum in the density of states[10]. The undoped state is a strongly correlated Mott insulator, and doping changes the state into a superconducting state[11]. To thoroughly understand the superconducting behavior, the electronic structure should be clearly elucidated. The band modification of the TBG sample with a relatively large twist angle was experimentally observed using nanometer-scale angle-resolved photoemission spectroscopy (nano-ARPES) measurements[12–14]. Very recently, nano-ARPES measurements of micrometer-scale TBG samples with a twist angle close to the magic-angle were performed, and the flat band almost at the Fermi energy was directly observed[15,16]. The next challenge is to obtain millimeter-scale TBG samples and to control the energy of the flat bands.

Here we report a possible solution to these challenges, which are revealed using a TBG sample fabricated by transferring millimeter-scale epitaxial graphene grown on SiC onto another epitaxial graphene on SiC. We found the large interlayer interaction in the 2.3° TBG sample from our ARPES measurement in more than 3×5 mm² area. In the magic-angle TBG sample, a flat band was directly observed at about $E = -0.37$ eV, indicating electron doping. Fabrication of the millimeter-scale TBG sample and direct observation of the flat band will expand the path to the realization of twistronics.

Results and discussion

Fabrication and basic characterization of the TBG sample. A schematic diagram of the sample preparation procedure is shown in Fig. 1a. Epitaxial monolayer graphene (EMLG) samples on SiC substrates with an area of 5×5 mm² were prepared by the thermal decomposition of SiC. EMLG on the SiC substrate 1 was exfoliated from the substrate using a deposited Au film and thermal release tape and transferred onto EMLG on the SiC substrate 2, according to a previously reported procedure[17]. After transferring graphene with a certain twist angle θ, the tape and the Au film were removed, and then the sample was annealed in a vacuum to remove surface contamination. In this study, we define the target twist angle as θ_t, and the angle based on the theoretical calculation as θ_c. The latter is compared with the experimental results, and this is a main method to measure the twist angle.

Figure 1b shows the Raman spectra of TBG with $\theta_t = 2.3°$ and the pristine EMLG. Additional features of the EMLG on SiC 1 and 2 are shown in Supplementary Note 1 and Supplementary Fig. S1. The spectra exhibited sharp G and 2D bands at around 1600 and 2700 cm⁻¹, respectively, indicating the high quality of the graphene. The broad features observed at 1300–1600 cm⁻¹ are due to the buffer layer under the epitaxial graphene. The 2D bands of TBG and EMLG had a full width at half maximum of about 74 and 35 cm⁻¹, respectively. An asymmetric shape of the 2D band in

TBG could be explained by the presence of bilayer graphene[18–20]. It is known that the 2D band is asymmetric in Bernal stacked bilayer graphene or in twisted bilayer graphene with a twist angle of less than 3°[21]. In addition, the spectrum in TBG had an additional peak on the right shoulder of the G band. This peak is called as the R′ band, which is frequently observed in TBG[22,23]. The position of this peak was at 1602 cm⁻¹, which suggests the small twist angle. Taking TBG into account, the broad 2D band can be explained by the two components due to the upper and the lower graphene layer, and actually, it was fitted by two Lorentzian curves at 2672 and 2716 cm⁻¹. The peak position of the 2D band in typical EMLG on SiC is about 2710 cm⁻¹, mainly due to the compressive strain originating from the substrate[24]. On the other hand, monolayer graphene without any strain or doping even on SiC has the 2D band at about 2670 cm⁻¹[25,26]. Thus, the present 2D peaks at 2672 and 2716 cm⁻¹ can be assigned to the transferred graphene without strain and the underlying EMLG, respectively.

Electronic structure of the large-θ TBG sample. In order to understand the electronic structure, we performed ARPES measurements of our TBG samples. The ARPES results of the TBG sample with the twist angle of $\theta_t = 2.3°$, which is the same sample as shown in Fig. 1b, are shown in Fig. 2. Figure 2a is the ARPES image at $k_y = 1.70$ Å⁻¹ around the K point in reciprocal space, taken at the center of the sample as shown by the blue dot in Fig. 2h. In Fig. 2b, the calculated band structure of TBG with $\theta_c = 2.9°$ without the interlayer interaction is overlaid. Figure 2c, d is the three-dimensional band structures of TBG and the schematic moiré Brillouin zone. Figure 2e–g is the ARPES images of k_x–k_y at $E = -0.2$ eV, E–k_y at $k_x = 0$ Å⁻¹, and E–k_y at $k_x = 0.09$ Å⁻¹, respectively. Two Dirac-type bands are clearly shown at different positions, as shown in Fig. 2a, e. The Dirac points of the faint (blue) and clear (red) bands are located at (k_x [Å⁻¹], k_y [Å⁻¹], E [eV]) = (0.000, −1.700, −0.270) and (0.086, −1.700, −0.200). The difference of 0.086 Å⁻¹ in k_x can be explained by the twist angle of $\theta_c = 2.9°$. Taking the escape depth of the photoelectrons into account, the clear and faint bands are probably due to the upper and lower graphene layers, respectively.

Interestingly, the clear band was strongly modified at the position where the two bands intersected, as shown by an arrow. It is clearly shown in Fig. 2b that the bandgap opens at the intersection of two bands. The same feature can also be recognized in Fig. 2g, as shown by an arrow. The illustrations of the bands in Fig. 2b, c are based on a tight-binding calculation without the interlayer interaction. The large bandgap opening indicates that the interlayer interaction was actually large. It should also be noted here that the target twist angle was $\theta_t = 2.3°$ and that the band structure can be well fitted by the twist angle $\theta_c = 2.9°$, indicating the small error range. Similar band modification was also observed in TBG with 3.5° as shown in Supplementary Note 3 and Supplementary Fig. S3.

We took similar ARPES images at different points on the sample, as shown in Fig. 2h. The observable area was about 3.5 × 5 mm², which is restricted by the sample holder of the ARPES experiment. Two bands and the bandgap were clearly observed at the positions as shown as red dots, while only one band could be observed at the two positions as shown as black dots. These results clearly indicated that TBG occurred over an area with a size of more than 3×5 mm² and from which the significant interlayer interaction could be obtained.

Electronic structure of the magic-angle (1.1°) TBG sample. The next target was the magic-angle TBG. Now the sample was obtained by the same procedure with the target angle of $\theta_t = 0.6$–1.0°, as shown in Fig. 3a. The ARPES image is shown in
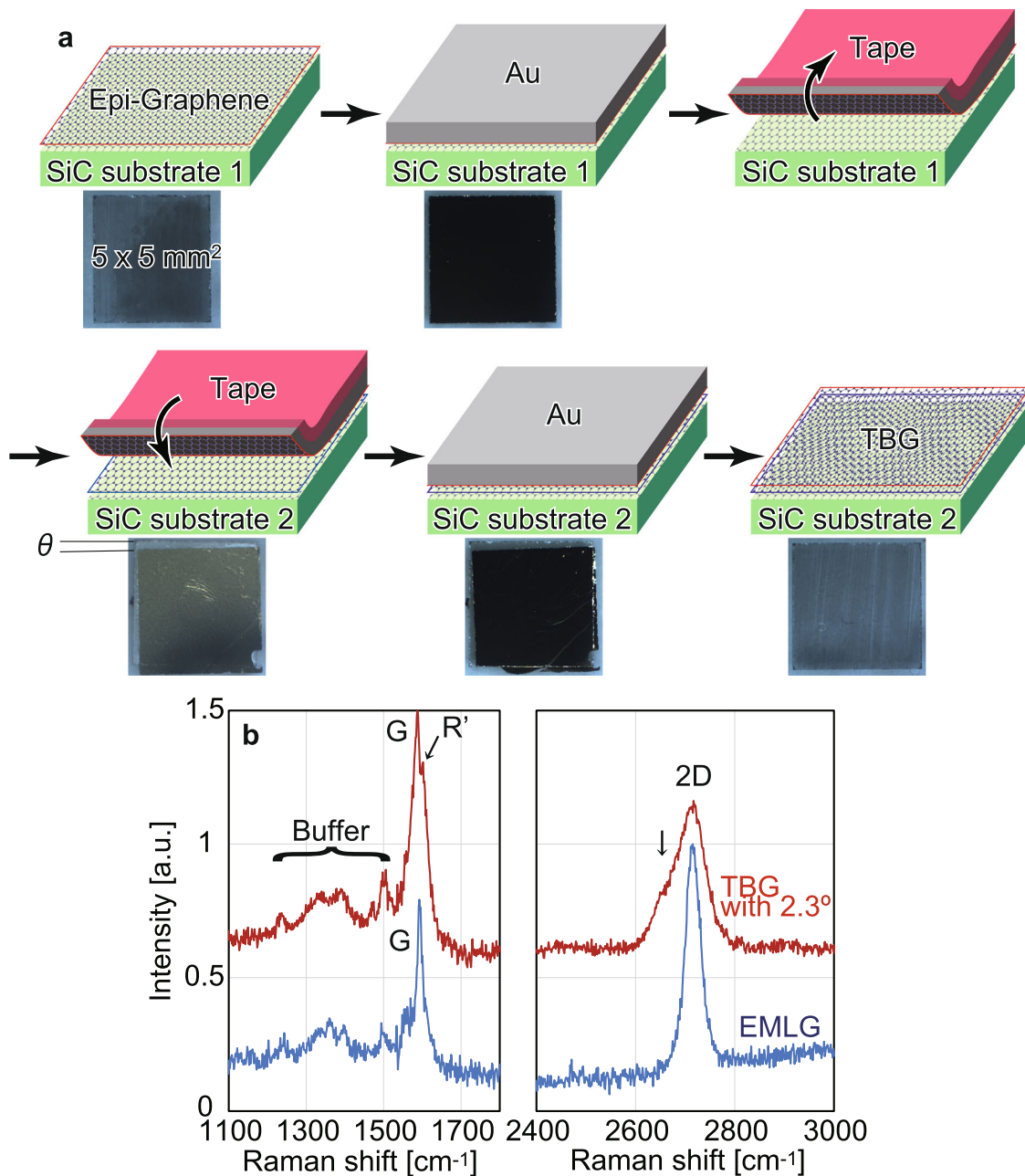
Fig. 1 TBG sample preparation. a Schematic diagram of the TBG sample preparation procedure. Au film was deposited onto EMLG on the SiC substrate 1. Graphene was exfoliated together with the Au film using a thermal release tape. It was then transferred with a twist angle onto the SiC substrate 2, which has EMLG on top. Optical microscope images during these procedures are also shown. The upper and lower graphene layers in TBG are illustrated in red and blue borders, and the buffer layer is shown translucently. After the transfer process, the sample was annealed at 400 °C for 2 h. In a high vacuum of about 1.5×10^{-5} Pa. **b** Raman spectra of TBG (red) and EMLG (blue). The spectra after subtracting the SiC substrate component are shown.

Fig. 3b. There seemed to be two or more bands which are close to each other. We estimated the twist angle to be about 1.1° from the comparison between the experimental results and the calculation, which will be shown below. One of the striking features of the ARPES image is the high density of states at −0.22 and −0.51 eV. Figure 3c is the intensity profile along the $k_x = 0.016$ Å^{-1} line in Fig. 3b. In addition to the states at −0.22 and −0.51 eV, another band at −0.37 eV was observed in between them, as shown by dotted lines in Fig. 3b, c. In Fig. 3e, the tight-binding band structure of $\theta_c = 1.1°$ TBG without the interlayer interaction is overlaid on the ARPES image. Two Dirac points in Fig. 3e locate at $(k_x$ [Å^{-1}], k_y [Å^{-1}], E [eV]) = (0.000, −1.700, −0.385) and (0.033, −1.700, −0.382). The k_x–k_y maps at different binding

energies are shown in Supplementary Notes 4, 5, Supplementary Figs. S4, S5, and Supplementary Movies 1, 2. Twist angle of 1.1° is supported by the observed agreement between ARPES constant energy images and the Dirac cone of 1.1° twisted upper and lower graphene layers as shown in Supplementary Fig. S5b–d. Interestingly, there seem to be additional bands shown in light blue and green in the k_x–k_y map in Supplementary Fig. S5. The position (k_x, k_y) of Dirac points of these bands cannot be explained by the period of the moiré superlattice nor by the 6√3 × 6√3R30 reconstruction of the SiC surface, which suggests a hidden symmetry of TBG, although their origin is not clear. Figure 3f is the spectral function of TBG for $\theta_c = 1.08°$, which is calculated by the effective continuum model (see Supplementary Note 6 and
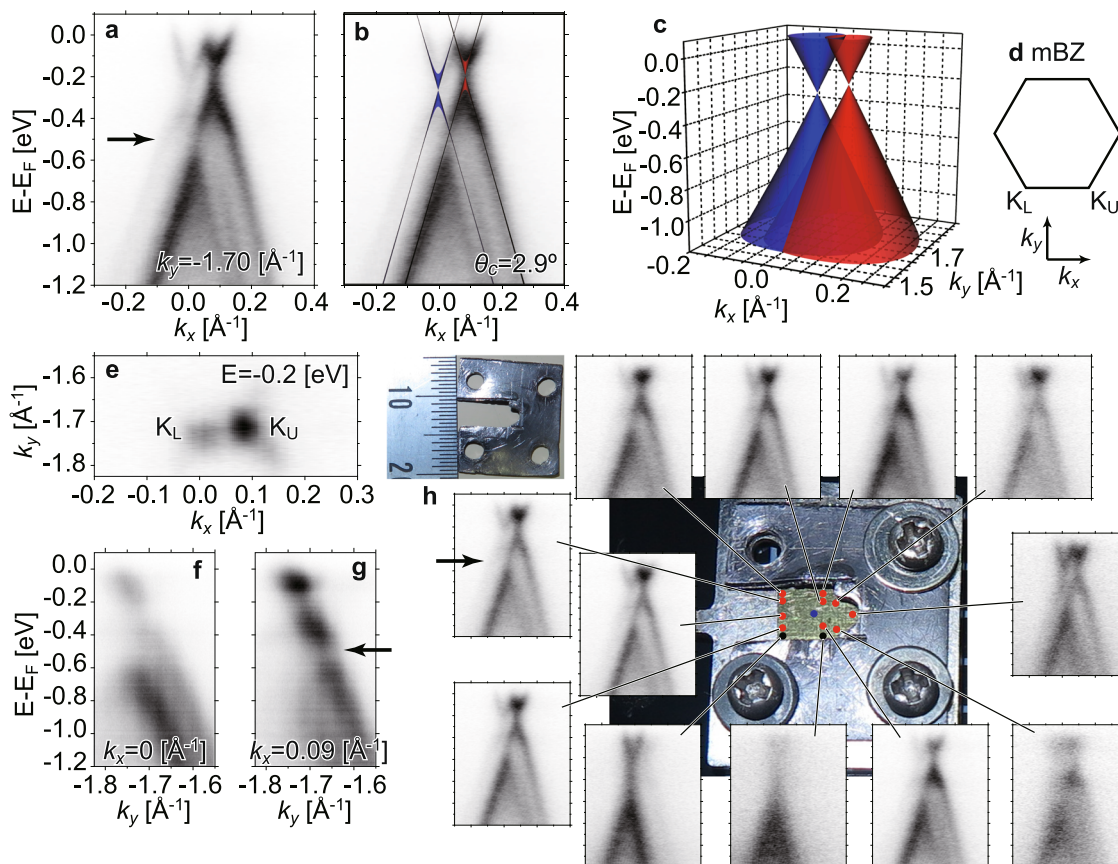
Fig. 2 ARPES results of TBG with large twist angle. a ARPES image of TBG sample, which is the same as shown in Fig. 1b. Two Dirac dispersions can be seen. The band modification is shown by an arrow. **b** The same ARPES image on which the schematic band structure with $\theta_c = 2.9°$ is overlaid. Blue and red bands correspond to the lower and upper graphene layers. **c** Three-dimensional model of the band structure of TBG calculated by a tight-binding scheme without the interlayer interaction. **d** Schematic diagram of the moiré Brillouin zone (mBZ). K_L and K_U represent the position of K points of the lower and upper graphene layers. **e–g** ARPES images of k_x–k_y at $E = -0.2$ eV, E–k_y at $k_x = 0$ Å^{-1}, and E–k_y at $k_x = 0.09$ Å^{-1}. **h** ARPES images taken at different locations, shown by dots in the optical micrograph of the sample and the sample holder. Horizontal and vertical scales in the images are the same as in **a**. The band modification could be observed on the position shown by red and blue dots, while it was not observed on the black dots. The size of the sample holder is also shown at the upper left.

Supplementary Fig. S6 for more information on this calculation)[27]. The flat band is clearly observed at $E = -0.37$ eV.

These calculations can readily explain the experimental results. For example, the bands shown by the red and blue arrows in Fig. 3b coincide with the corresponding bands in Fig. 3e, f. Figure 3d is the intensity profile of Fig. 3f along the $k_x = 0.016$ Å^{-1} line. By comparing this calculation and the experimental results, we can assign the high-intensity bands at -0.22 and -0.51 eV to the peaks in Fig. 3d. Another band at -0.37 eV shown by the center dotted line in Fig. 3c could then be identified as the strongest peak in Fig. 3d, i.e., the flat band. The flat band was experimentally visible only in the narrow k_x region -0.023 to 0.060 Å^{-1}, while it was present more widely along k_x in the calculation. This is consistent with the recent reports on the flat band in magic-angle TBG[15,16]. Another band, indicated by the black arrow, which is the replica band due to the moiré superlattice symmetry, could not be observed experimentally, probably due to a weak intensity or some other as yet unknown reason.

Asymmetrical doping in TBG. Here, we discuss the point that the Dirac energy and its difference between the upper and lower layer differed with the twist angle. The Dirac energy of the upper layer E_{DU}, lower layer E_{DL}, and their difference ΔE of TBG with $\theta = 1.1$, 2.9, and 3.5 were (E_{DU} [eV], E_{DL} [eV], ΔE [eV]) =

$(-0.382, -0.385, 0.003)$, $(-0.20, -0.27, 0.07)$, and $(-0.18, -0.24, 0.06)$, respectively. The band of the lower layer seemed to be more electron-doped. We have also performed ARPES measurements of exfoliated EMLG which was on Au/tape (e-EMLG/Au/tape), and of this graphene transferred onto buffer/SiC (t-EMLG/buf/SiC) as shown in Supplementary Note 7 and Supplementary Fig. S7. Their Dirac energies were about -0.04 and -0.20 eV. This result indicates that the origin of electron doping is not the substitution of carbon in graphene by the different elements, but the effect of the buffer/SiC substrate. We here recall that the Dirac energies of EMLG on SiC and epitaxial bilayer graphene on SiC were about -0.40 and -0.30 eV, respectively[19,28–30]. The widely accepted origin of doping is the polarization of the hexagonal SiC substrate and the presence of the buffer layer[31,32]. Bilayer graphene is less electron-doped, which is caused by the screening of the substrate effect due to the larger distance from the substrate. Differences in the Dirac energies of the upper and lower graphene layers in the present TBG are probably attributed to the same screening effect. In other words, the substrate potential induced the asymmetrical doping in TBG.

We note that ΔE differed with the twist angle. ΔE was quite small in the magic-angle TBG, but was larger in TBG with a larger twist angle, although its change was not systematic. This result suggests that the screening effect was small in the small twist angle TBG, suggesting a strong interlayer interaction in
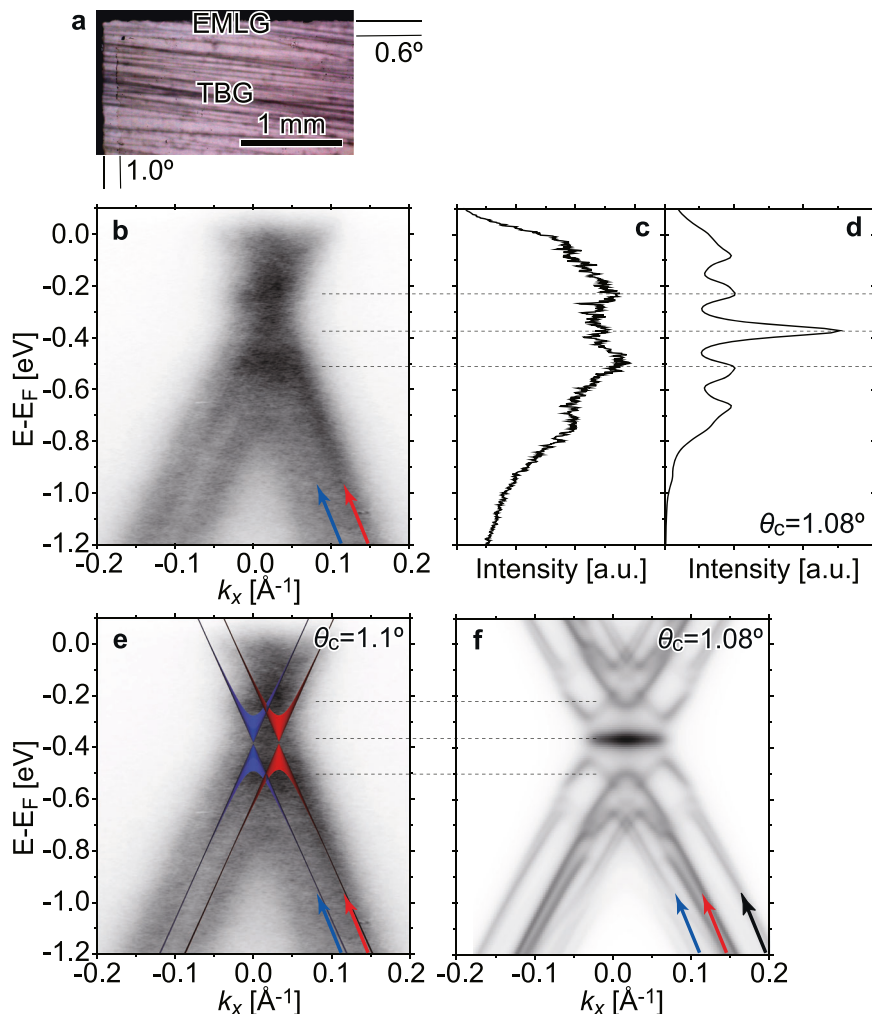
Fig. 3 ARPES images of TBG near the magic-angle. a Optical micrograph with highlighted contrast of the TBG sample. Horizontal striations are scratches of the substrate rear. **b** ARPES image at the K points of TBG. **c**, **d** Energy dispersion curve along the $k_x = 0.016$ [Å^{-1}] line in **b**, **f**. **e** ARPES image together with the overlaid schematic TBG band structure with $\theta_c = 1.1°$. Band structures without the interlayer interaction are shown. Blue and red bands correspond to the lower and upper graphene layers. **f** Single-particle spectral function of TBG with $\theta_c = 1.08°$, calculated by the effective continuum model.

magic-angle TBG. Interlayer interaction and deformation within the layers around the magic-angle may affect this result[33], although it should be further investigated. It should be emphasized here that the electron-doped nature of graphene on SiC helped to observe a flat band of both the higher and lower energy regions, compared to the previous reports where only the lower energy region was observed[15,16]. A similar electron-doped flat band structure was observed in non-twisted bilayer graphene on SiC[34]. In this case, the mechanism of the flat band formation at higher energy was considered to be the relative biasing of only one sublattice against other sublattices in the bilayer. This was also achieved by the strong interaction with the buffer/SiC substrate. In both cases, the substrate potential plays important roles in the electronic structure. In the present study, the position of the flat band was between the π and π' bands, which is usually found in magic-angle TBG. Electrical measurements of millimeter-scale magic-angle TBG will be our future work.

Methods

Sample preparation. We used on-axis 4H-SiC (0001) substrates. The substrate was cut into 5×5 mm^2 pieces, and the surface was polished chemical-mechanically. The substrates were cleaned ultrasonically in ethanol and acetone. The surface native oxide was removed by immersing the substrates in HF solution, followed by cleaning in deionized water. EMLG samples were prepared by heating the substrate under atmospheric pressure of Ar at 1700 °C. Atomic force

microscope topography and phase images were taken to reveal the surface morphology and the graphene thickness distribution (see Supplementary Note 1, 2 and Supplementary Figs. S1, S2). Raman spectroscopy measurements were performed using a Renishaw inVia Reflex with a 532 nm excitation laser with a spot size of about 1 μm to check the structural features of the EMLG and TBG.

Transfer process. Graphene transfer was done using the same procedure described in the previous report[17]. As the first step of the transfer, graphene was coated with a layer of Au with a thickness of 200 nm. Then, the Au/graphene film was exfoliated from the substrate using thermal release tape. This tape/Au/graphene was put on another EMLG sample, and the tape was removed. Finally, the Au thin film was etched away using I$_2$/KI solution. The samples were annealed at 400 °C for 2 h. in a high vacuum of 1.5×10^{-5} Pa to clean the surface.

Sample characterization. The number of transferred graphene layers was indirectly estimated by Raman spectroscopy. The surface features of the TBG sample were investigated by low-energy electron diffraction (LEED) and low-energy electron microscopy (LEEM). The electronic structure was observed by ARPES at the Aichi Synchrotron Radiation Center. The ARPES experiment was performed at room temperature using a 70 eV photon energy with about 150×70 μm^2 spot size.

Calculations. To simulate theoretically the ARPES image, we obtained the spectral weight distribution by calculation of the single-particle spectral function. For the calculation of the spectral function, we used the continuum model of TBG at twist angle $\theta_c = 1.08°$ (for details, see Supplementary Note 6 and Supplementary Fig. S6).

Data availability

Data are available from the corresponding author upon reasonable request.

References

1. Lopes dos Santos, J. M. B., Peres, N. M. R. & Castro Neto, A. H. Graphene bilayer with a twist: electronic structure. *Phys. Rev. Lett.* **99**, 256802 (2007).
2. Lucian, A. et al. Single-layer behavior and its breakdown in twisted graphene layers. *Phys. Rev. Lett.* **106**, 126802 (2011).
3. Suarez Morell, E., Correa, J. D., Vargas, P., Pacheco, M. & Barticevic, Z. Flat bands in slightly twisted bilayer graphene: tight-binding calculations. *Phys. Rev. B* **82**, 121407(R) (2010).
4. Rong, Z. Y. & Kuiper, P. Electronic effects in scanning tunneling microscopy: Moiré pattern on a graphite surface. *Phys. Rev. B* **48**, 17427 (1993).
5. Park, C.-H., Yang, L., Son, Y.-W., Cohen, M. L. & Louie, S. G. New generation of massless Dirac fermions in graphene under external periodic potentials. *Phys. Rev. Lett.* **101**, 126804 (2008).
6. Yankowitz, M. et al. Emergence of superlattice Dirac points in graphene on hexagonal boron nitride. *Nat. Phys.* **8**, 382 (2012).
7. Chizhova, L. A., Libisch, F. & Burgdoerfer, J. Graphene quantum dot on boron nitride: Dirac cone replica and Hofstadter butterfly. *Phys. Rev. B* **90**, 165404 (2014).
8. Celis, A. et al. Superlattice-induced minigaps in graphene band structure due to underlying one-dimensional nanostructuration. *Phys. Rev. B* **97**, 195410 (2018).
9. Carr, S. et al. Twistronics: manipulating the electronic properties of two-dimensional layered structures through their twist angle. *Phys. Rev. B* **95**, 075420 (2017).
10. Cao, Y. et al. Unconventional superconductivity in magic-angle graphene superlattices. *Nature* **556**, 43 (2018).
11. Cao, Y. et al. Correlated insulator behaviour at half-filling in magic-angle graphene superlattices. *Nature* **556**, 80 (2018).
12. Ohta, T. et al. Evidence for interlayer coupling and moiré periodic potentials in twisted bilayer graphene. *Phys. Rev. Lett.* **109**, 186807 (2012).
13. Kandyba, V., Yablonskikh, M. & Barinov, A. Spectroscopic characterization of charge carrier anisotropic motion in twisted few-layer graphene. *Sci. Rep.* **5**, 16388 (2015).
14. Razado-Colambo et al. NanoARPES of twisted bilayer graphene on SiC: absence of velocity renormalization for small angles. *Sci. Rep.* **6**, 27261 (2016).
15. Utama, M. I. B. et al. Visualization of the flat electronic band in twisted bilayer graphene near the magic angle twist. *Nat. Phys.* **17**, 184 (2021).
16. Lisi, S. et al. Observation of flat bands in twisted bilayer graphene. *Nat. Phys.* **17**, 189 (2021).
17. Kim, J. et al. Layer-resolved graphene transfer via engineered strain layers. *Science* **342**, 833 (2013).
18. Fromm, F. et al. Contribution of the buffer layer to the Raman spectrum of epitaxial graphene on SiC(0001). *N. J. Phys.* **15**, 043031 (2013).
19. Kusunoki, M., Norimatsu, W., Bao, J., Morita, K. & Starke, U. Growth and features of epitaxial graphene on SiC. *J. Phys. Soc. Jpn.* **84**, 121014 (2015).
20. Norimatsu, W. & Kusunoki, M. Structural features of epitaxial graphene on SiC {0001} surfaces. *J. Phys. D Appl. Phys.* **47**, 094017 (2014).
21. Kim, K. et al. Raman spectroscopy study of rotated double-layer graphene: misorientation-angle dependence of electronic structure. *Phys. Rev. Lett.* **108**, 246103 (2012).
22. Carozo, V. et al. Raman signature of graphene superlattices. *Nano Lett.* **11**, 4527 (2011).
23. Eliel, G. S. N. et al. Intralayer and interlayer electron – phonon interactions in twisted graphene heterostructures. *Nat. Commun.* **9**, 1221 (2018).
24. Fromm, F., Wehrfritz, P., Hundhausen, M. & Seyller, T. H. Looking behind the scenes: Raman spectroscopy of top-gated epitaxial graphene through the substrate. *N. J. Phys.* **15**, 113006 (2013).
25. Lee, J. E. et al. Optical separation of mechanical strain from charge doping in graphene. *Nat. Commun.* **3**, 1024 (2012).
26. Bao, J. et al. Synthesis of freestanding graphene on SiC by a rapid-cooling technique. *Phys. Rev. Lett.* **117**, 205501 (2016).
27. Koshino, M. et al. Maximally localized Wannier orbitals and the extended Hubbard model for twisted bilayer graphene. *Phys. Rev. X* **8**, 031087 (2018).
28. Bostwick, A., Ohta, T., Seyller, T. H., Horn, K. & Rotenberg, E. Quasiparticle dynamics in graphene. *Nat. Phys* **3**, 36 (2007).
29. Ohta, T., Bostwick, A., Seyller, T. H., Horn, K. & Rotenberg, E. Controlling the electronic structure of bilayer graphene. *Science* **313**, 951 (2006).
30. Riedl, C., Coletti, C. & Starke, U. Structural and electronic properties of epitaxial graphene on SiC(0001): a review of growth, characterization, transfer doping and hydrogen intercalation. *J. Phys. D Appl. Phys.* **43**, 374009 (2010).
31. Ristein, J., Mammadov, S. & Seyller, T. H. Origin of doping in Quasi-free-standing graphene on silicon carbide. *Phys. Rev. Lett.* **108**, 246104 (2012).
32. Mammadov, S. et al. Polarization doping of graphene on silicon carbide. *2D Mater.* **1**, 035003 (2014).
33. Kazmierczak, N. P. et al. Strain fields in twisted bilayer graphene. *Nat. Mater.* **20**, 956 (2021).
34. Marchenko, D. et al. Extremely flat band in bilayer graphene. *Sci. Adv.* **4**, eaau0059 (2018).

Acknowledgements

Author contributions

K.S., K.Q., D.L., J.K., and T.M. prepared the TBG samples. K.S., N.H., T.I., and W.N. performed the ARPES measurements. K.N. and K.W. carried out the theoretical calculations. H.H. observed TBG samples using LEED. W.N. supervised the project. K.S., T.I., N.M., M.T., M.M., T.M., D.L., J.K., K.W., H.H., and W.N. discussed the experimental and theoretical results. All authors contributed to writing the manuscript.

Competing interests

The authors declare no competing interests.

Additional information